

WaDi: Weight Direction-aware Distillation for One-step Image Synthesis

Lei Wang¹, Yang Cheng¹, Senmao Li¹, Ge Wu¹, Yaxing Wang^{1,3†}, Jian Yang^{1,2†}

¹PCA Lab, VCIP, College of Computer Science, Nankai University

²PCA Lab, School of Intelligence Science and Technology, Nanjing University

³ NKIARI, Shenzhen Futian

{scitop1998, cyrene0613, senmaonk, gewu.nku}@gmail.com, {yaxing, csjyang}@nankai.edu.cn

Code: <https://github.com/gudaochangsheng/WaDi>



Figure 1. One-step generated images using our proposed method WaDi (*i.e.*, SD 2.1).

Abstract

Despite the impressive performance of diffusion models such as Stable Diffusion (SD) in image generation, their slow inference limits practical deployment. Recent works accelerate inference by distilling multi-step diffusion into one-step generators. To better understand the distillation mechanism, we analyze U-Net/DiT weight changes between one-step students and their multi-step teacher counterparts. Our analysis reveals that changes in weight direction significantly exceed those in weight norm, highlighting it as the key factor during distillation. Motivated by this insight, we propose the **Low-rank Rotation of weight Direction (LoRaD)**, a parameter-efficient adapter tailored to one-step diffusion distillation. LoRaD is designed to model these structured direc-

tional changes using learnable low-rank rotation matrices. We further integrate LoRaD into Variational Score Distillation (VSD), resulting in **Weight Direction-aware Distillation (WaDi)**—a novel one-step distillation framework. WaDi achieves state-of-the-art FID scores on COCO 2014 and COCO 2017 while using only approximately 10% of the trainable parameters of the U-Net/DiT. Furthermore, the distilled one-step model demonstrates strong versatility and scalability, generalizing well to various downstream tasks such as controllable generation, relation inversion, and high-resolution synthesis.

1. Introduction

Diffusion models (DMs) [15, 55, 58] have received considerable attention for their ability to generate high-quality

[†]Corresponding authors.

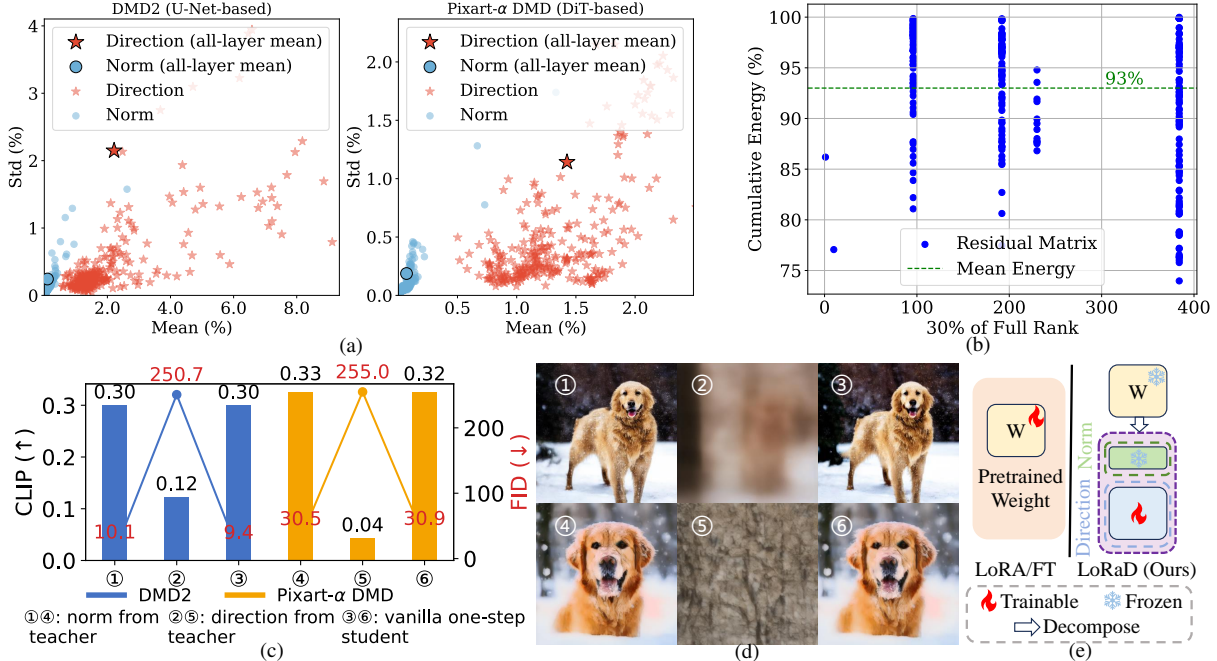


Figure 2. Motivational analysis of our method. (a) Differences in weight norm and direction between the one-step student and the teacher model. See [Suppl. E](#) for details and additional examples. (b) SVD analysis of the residual matrix for DMD2. (c) Replacing the one-step model’s norm with that of the multi-step model has little effect (①, ④); replacing the direction severely degrades generation quality (②, ⑤). (d) Qualitative examples corresponding to (c). (e) Illustration of LoRaD.

and diverse content. Thus, they are widely applied to tasks such as text-to-image [30, 49, 50, 74] generation, text-to-video [24, 26, 67, 78] generation, and image-to-video [2, 19, 44, 63] generation. However, the reliance of DMs on multiple sampling steps leads to high computational cost and slow inference. To address this, recent distillation methods reduce the number of steps to a few [3, 40] or even one [8, 31, 48]. Interestingly, during distillation, we find that the weight norm remains relatively small across layers, while the direction shows larger variations when reparameterizing weights into *norm* and *direction* for both teacher and student generators.

Inspired by the weight reparameterization [34, 52], we adopt a similar decomposition to analyze weight changes in diffusion distillation. To begin our analysis, we examine weight updates between state-of-the-art (SOTA) one-step models (e.g., DMD2 [72] and Pixart- α DMD [73]) and their corresponding multi-step counterparts (e.g., SD 1.5 [49] and Pixart- α [4]). As shown in Fig. 2 (a) (left), in U-Net-based architectures, the weight norm remains nearly stable across layers, with a mean and standard deviation (STD) of 0.1% and 0.2%, respectively. In contrast, the weight direction exhibits a much more pronounced change, with a mean of 2.2% and STD of 2.1%, corresponding to ratios of 22 \times and 10 \times those of the norm. A similar trend is observed in DiT-based architectures (see Fig. 2 (a) (right)). These observations suggest that the weight direction may carry richer and more sensitive information than the norm in distillation. Further,

if the direction indeed accounts for the primary information differences, we ask whether these differences exhibit a structured pattern. To this end, we perform SVD on the residual matrix—the difference between the one-step and multi-step direction matrices—and find that retaining 30% of its rank recovers 93% of the information, highlighting its low-rank nature (see Fig. 2 (b)).

To quantify the impact of these two components, we conduct a controlled ablation study by selectively replacing either the norm or direction of the one-step model with that from the multi-step teacher (see Fig. 2 (d)). As shown in Fig. 2 (c), substituting the norm leads to negligible performance change (e.g., DMD2: +0.7 FID, unchanged CLIP), whereas substituting the direction causes severe degradation (e.g., DMD2: +241.3 FID, -0.18 CLIP). These findings suggest that the weight direction plays a primary role in distillation, while variation in the norm appears comparatively minor. One possible explanation is that initializing the student with teacher weights aligns the initial norm, and weight decay during training further constrains norm drift [35]; the distillation signal then acts mainly through adjustments in the weight direction to reduce representational discrepancy [52]. Taken together, these results indicate that **direction reconstruction is a key factor underlying performance improvement in distillation**.

The distillation methods mentioned above can be broadly categorized into two types: full fine-tuning (FT) and Low-Rank Adaptation (LoRA) [16]-based fine-tuning. However,

they directly update the model parameters while optimizing both norm and direction. The changes in norm and direction differ, with norm showing minimal variation and directions experiencing significant changes, which increases the optimization difficulty due to the strong coupling between them. Furthermore, both FT and LoRA face issues of slow convergence [9, 21], instability [12, 13], and overfitting [1, 20], further complicating the optimization process.

To address the above challenges, we propose Low-rank Rotation of weight Direction (LoRaD) (see Fig. 2 (e)), which adjusts the direction of pre-trained weights via learnable rotation matrices. Given the structured nature (*i.e.*, low-rank property) of directional changes, the rotation angles are parameterized as the product of two low-rank matrices to further reduce the number of learnable parameters. We integrate LoRaD into Variational Score Distillation (VSD) [65] and introduce Weight Direction-aware Distillation (WaDi), a novel one-step text-to-image distillation framework. Experiments on the COCO 2014 [32] and COCO 2017 [32] datasets show that WaDi achieves SOTA FID scores, outperforming all existing one-step generation methods. This was accomplished by optimizing only the direction, which reduced the difficulty of distillation, while using only about **10%** of the U-Net parameters as trainable components—greatly enhancing parameter efficiency. Furthermore, we apply WaDi to downstream tasks including controllable generation, relation inversion, high-resolution synthesis, and image customization, demonstrating its acceleration capability and broad applicability. Our contributions are summarized as follows:

- We conduct an in-depth analysis of weight changes in U-Net between multi-step and one-step generation models, which points to weight-direction adjustment as a key driver of one-step distillation. This provides a new theoretical perspective for efficient distillation.
- We propose a novel distillation framework for one-step text-to-image generation, named WaDi, which employs LoRaD to model weight directions via low-rank rotations, effectively guiding the student model to align with the teacher distribution.
- WaDi is evaluated on the COCO dataset and several downstream tasks. Both qualitative and quantitative results demonstrate that WaDi significantly improves inference efficiency while achieving substantial gains in image quality.

2. Related Work

Diffusion models. Diffusion models [11, 15, 17, 18, 55, 57, 58, 69] excel in image generation, but pixel-space computation imposes a heavy computational burden. To improve efficiency, Rombach et al. [49] introduced Latent Diffusion Models (LDM), shifting denoising to latent space. However, existing text-guided methods [30, 46, 49, 50, 74] are still

slow due to multi-step generation. While most use a U-Net backbone, Diffusion Transformer (DiT) [45] replaces it with a Transformer for better scalability, advancing text-to-image generation [4–6, 10]. Despite improvements, iterative denoising remains a slow process. Recently, many acceleration methods have emerged.

Diffusion model acceleration. The existing acceleration methods can be divided into training-free and training-based approaches. *Training-free acceleration methods* for diffusion models fall into two main categories. The first method, which reduces redundant computation through caching [28, 42, 53, 66], is exemplified by Faster Diffusion [28]. The second method uses high-order solvers [33, 37, 38, 56, 75], such as DDIM [56] and DPM-Solver [37, 38], to reduce the number of sampling steps. However, the acceleration effects of these two methods are limited, so training-based methods have received more attention.

Training-based acceleration methods can be broadly categorized into four groups: consistency distillation (CD), progressive distillation (PD), diffusion-GAN distillation, and variational score distillation (VSD). CD [25, 39, 40, 48, 59, 64] learns trajectory-level consistency for faster sampling but often suffers from low image fidelity. PD [48, 51] reduces steps in stages, introducing significant training overhead. Diffusion-GAN distillation [23, 31, 41, 70], such as Diffusion2GAN [23], enhances fidelity by distilling multi-step diffusion into a GAN. VSD adopts a dual-teacher strategy for distribution alignment [8, 43, 72, 73, 76]. SwiftBrush [43] achieves one-step, image-free generation. SwiftBrushv2 [8] leverages model ensembling, while DMD [73] employs a regression loss to further improve performance. DMD2 [72] extends VSD to few-step generation and underpins recent text-to-video acceleration frameworks [54, 71].

However, existing training-based methods commonly use FT or LoRA, which can increase optimization difficulty. We find that directional changes are generally more influential in distillation. Therefore, we propose WaDi, which leverages LoRaD to focus on modeling directional rotations.

3. Method

We first provide a brief overview of Variational Score Distillation (VSD) in Section 3.1, which serves as the foundation of our work. Motivated by the observation that weight direction changes play a key role in distillation, we introduce a *Low-rank Rotation of weight Direction* (LoRaD) module in Section 3.2 (See *Suppl. D* for more theoretical explanation.). Finally, we integrate LoRaD into the VSD to form our proposed distillation framework, *Weight Direction-aware Distillation* (WaDi).

3.1. Preliminary

Latent Diffusion Models (LDM) [49] perform the diffusion process in a low-dimensional latent space, which improves

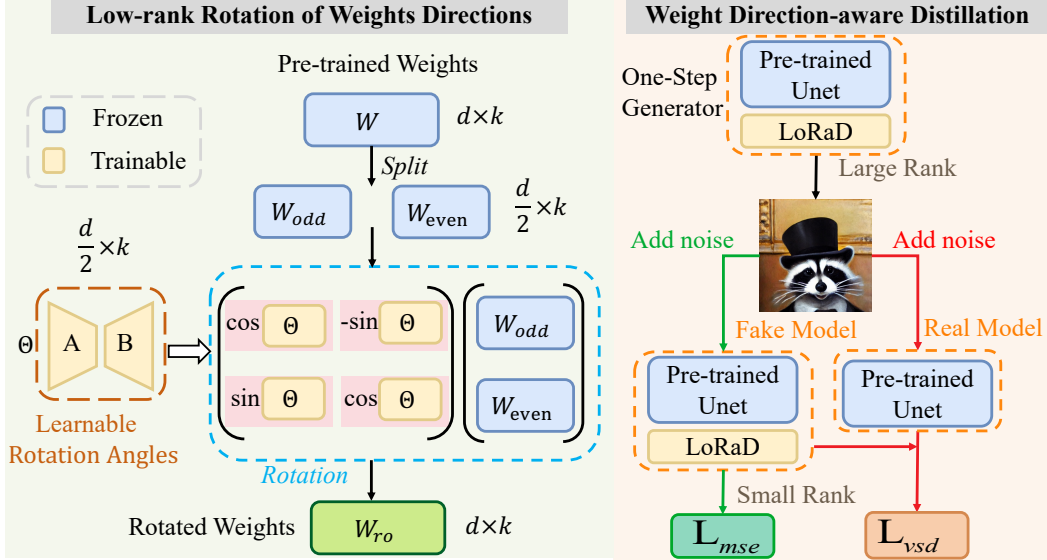


Figure 3. (Left) Detailed architecture of the Low-rank Rotation of weight Direction (LoRaD) module. The LoRaD rotates the pre-trained weight directions using learnable low-rank rotation angles. (Right) Overview of the Weight Direction-aware Distillation (WaDi) framework.

computational efficiency. The training objective of LDM can be formulated as:

$$\mathcal{L}_{mse} = \min_{\varphi} \mathbb{E}_{t, \epsilon, c} \|\epsilon_{\varphi}(z_t, c, t) - \epsilon\|_2^2, \quad (1)$$

where $\epsilon \sim \mathcal{N}(0, I)$ is Gaussian noise, z_t is the latent variable at timestep t , and c denotes the condition (e.g., prompt) used to guide image generation. $\epsilon_{\varphi}(z_t, c, t)$ is the noise predicted by the model parameterized by φ .

Variational Score Distillation (VSD) [65] was initially proposed for text-to-3D generation to address issues such as oversaturation and reduced diversity. It was subsequently extended to 2D text-to-image generation in methods such as Swiftbrush [43], DMD [72, 73], and SiD [76, 77], enabling one-step generation. The training objective of VSD is formulated as:

$$\nabla_{\lambda} \mathcal{L}_{vsd} = \mathbb{E}_{t, \epsilon, c} \left[\omega(t) (\epsilon_{\psi}(z_t, c, t) - \epsilon_{\phi}(z_t, c, t)) \frac{\partial G_{\lambda}(z_{init}, c)}{\partial \lambda} \right]. \quad (2)$$

where $\omega(t)$ is a time-dependent weighting term, ϵ_{ψ} is the real model parameterized by ψ , ϵ_{ϕ} is the fake model parameterized by ϕ , and G_{λ} is the one-step generator parameterized by λ , with $z_{init} \sim \mathcal{N}(0, I)$ as its input noise. Additionally, ϵ_{ϕ} is trained using Eq. (1). VSD alternates between updating ϵ_{ϕ} and G_{λ} until convergence.

3.2. Low-rank Rotation of Weight Direction

Analyzing the weight changes between multi-step U-Net models and their one-step counterparts suggests notable directional shifts with relatively small changes in norm. Motivated by this, we propose Low-rank Rotation of weight Direction (LoRaD) (see Fig. 3 (left)), which updates weights

by learning rotations that alter only their directions. Furthermore, we observe that the changes in weight direction exhibit a low-rank structure (see Fig. 2 (b)). To exploit this property and reduce the overhead of full-rank modeling, which introduces additional parameters equivalent to 50% of the original weights, we adopt the low-rank decomposition strategy of LoRA [16]. Starting from the 2D case ($d = 2$), given a weight vector $\alpha \in \mathbb{R}^d$, we apply a 2D rotation matrix as follows:

$$\alpha_{ro} = \begin{pmatrix} \cos \theta & -\sin \theta \\ \sin \theta & \cos \theta \end{pmatrix} \begin{pmatrix} \alpha^{(1)} \\ \alpha^{(2)} \end{pmatrix}, \quad (3)$$

where α_{ro} is the rotated weight vector. Inspired by the Rotary Position Embedding (RoPE) [60], which generalizes the 2D case to any even dimension d , we apply a different rotation matrix[†] to each column of the pre-trained weight matrix $W \in \mathbb{R}^{d \times k}$:

$$W_{ro} = [R_{\Theta,1}^d W_{.,1}, R_{\Theta,2}^d W_{.,2}, \dots, R_{\Theta,k}^d W_{.,k}], \quad (4)$$

where the rotation matrices $R_{\Theta} = \{R_{\Theta,i}^d\}_{i=1}^k$ are defined as:

$$R_{\Theta,i}^d = \begin{pmatrix} \cos \theta_{1,i} & -\sin \theta_{1,i} & 0 & 0 & \dots & 0 & 0 \\ \sin \theta_{1,i} & \cos \theta_{1,i} & 0 & 0 & \dots & 0 & 0 \\ 0 & 0 & \cos \theta_{2,i} & -\sin \theta_{2,i} & \dots & 0 & 0 \\ 0 & 0 & \sin \theta_{2,i} & \cos \theta_{2,i} & \dots & 0 & 0 \\ \vdots & \vdots & \vdots & \vdots & \ddots & \vdots & \vdots \\ 0 & 0 & 0 & 0 & \dots & \cos \theta_{\frac{d}{2},i} & -\sin \theta_{\frac{d}{2},i} \\ 0 & 0 & 0 & 0 & \dots & \sin \theta_{\frac{d}{2},i} & \cos \theta_{\frac{d}{2},i} \end{pmatrix}, \quad (5)$$

where $\Theta = \{\theta_j\}_{j=1}^{\frac{d}{2}} \in \mathbb{R}^{\frac{d}{2} \times k}$.

[†]We do not need to explicitly separate the norm matrix, as rotations do not affect norm.

Given the sparsity of $R_{\Theta,i}^d$ in Eq. (5), the matrix-vector multiplication $R_{\Theta,i}^d W_{\cdot,i} \in \mathbb{R}^d$ can be computed efficiently as:

$$R_{\Theta,i}^d W_{\cdot,i} = \begin{pmatrix} W_{\cdot,i}^{(1)} \\ W_{\cdot,i}^{(2)} \\ W_{\cdot,i}^{(3)} \\ W_{\cdot,i}^{(4)} \\ \vdots \\ W_{\cdot,i}^{(d-1)} \\ W_{\cdot,i}^{(d)} \end{pmatrix} \odot \begin{pmatrix} \cos \theta_{1,i} \\ \cos \theta_{1,i} \\ \cos \theta_{2,i} \\ \cos \theta_{2,i} \\ \vdots \\ \cos \theta_{\frac{d}{2},i} \\ \cos \theta_{\frac{d}{2},i} \end{pmatrix} + \begin{pmatrix} W_{\cdot,i}^{(1)} \\ W_{\cdot,i}^{(2)} \\ W_{\cdot,i}^{(3)} \\ W_{\cdot,i}^{(4)} \\ \vdots \\ W_{\cdot,i}^{(d-1)} \\ W_{\cdot,i}^{(d)} \end{pmatrix} \odot \begin{pmatrix} -\sin \theta_{1,i} \\ \sin \theta_{1,i} \\ -\sin \theta_{2,i} \\ \sin \theta_{2,i} \\ \vdots \\ -\sin \theta_{\frac{d}{2},i} \\ \sin \theta_{\frac{d}{2},i} \end{pmatrix}, \quad (6)$$

where \odot denotes element-wise multiplication. This implementation leverages the sparsity of the rotation matrix, allowing the computation to be performed using only element-wise operations, thus significantly reducing the computational cost.

Furthermore, since the rotation matrices in Eqs. (5) and (6) are block-diagonal with independent 2×2 submatrices, the computation can be efficiently implemented as a parallel application of multiple 2×2 rotations across odd-even index pairs. As shown in Fig. 3 (left), we split the d -dimensional space of the pre-trained weight matrix $W \in \mathbb{R}^{d \times k}$ into $\frac{d}{2}$ subspaces and rotate each independently. By separating the odd and even rows of W , we define:

$$\begin{aligned} W_{\text{odd}} &= \left(W^{(1)}, W^{(3)}, \dots, W^{(d-1)} \right)^T, \\ W_{\text{even}} &= \left(W^{(2)}, W^{(4)}, \dots, W_{\cdot,i}^{(d)} \right)^T, \end{aligned} \quad (7)$$

resulting in two matrices $W_{\text{odd}} \in \mathbb{R}^{\frac{d}{2} \times k}$ and $W_{\text{even}} \in \mathbb{R}^{\frac{d}{2} \times k}$.

The resulting parallel 2×2 rotations over each odd-even row pair can be expressed compactly as:

$$W_{ro} = R_{\Theta} W = \begin{bmatrix} \cos \Theta & -\sin \Theta \\ \sin \Theta & \cos \Theta \end{bmatrix} \begin{bmatrix} W_{\text{odd}} \\ W_{\text{even}} \end{bmatrix}, \quad (8)$$

where $W_{ro} \in \mathbb{R}^{d \times k}$ is the rotated weight matrix, and $\Theta \in \mathbb{R}^{\frac{d}{2} \times k}$ is the learnable rotation angle parameter matrix. To further reduce the number of trainable parameters, we apply low-rank decomposition to Θ , inspired by LoRA [16], as follows:

$$\Theta = AB, \quad (9)$$

where $A \in \mathbb{R}^{\frac{d}{2} \times r}$ and $B \in \mathbb{R}^{r \times k}$ are low-rank parameter matrices with rank r . Finally, Eq. (8) can be rewritten as:

$$W_{ro} = R_{\Theta} W = R_{AB} W = \begin{bmatrix} \cos AB & -\sin AB \\ \sin AB & \cos AB \end{bmatrix} \begin{bmatrix} W_{\text{odd}} \\ W_{\text{even}} \end{bmatrix}. \quad (10)$$

3.3. Weight Direction-aware Distillation

To fully leverage the directional characteristics observed in distillation, we integrate LoRaD into the VSD. This yields

a direction-aware distillation framework, which we term Weight Direction-aware Distillation (WaDi). As illustrated in Fig. 3 (right), WaDi employs a pre-trained diffusion model ϵ_{ψ} as the teacher (real model) and introduces a trainable fake model ϵ_{ϕ} (initialized from ϵ_{ψ}) to approximate the teacher’s distribution. The final student model (one-step generator) G_{λ} , also initialized from ϵ_{ψ} , is trained to synthesize high-quality images in one-step. See *Suppl. F.3* for algorithm details.

To enhance alignment with the real distribution, we apply LoRaD to both the student and fake models. Specifically, the one-step generator $G_{\lambda_{\Theta^l}}$ incorporates a high-rank rotation matrix Θ^l to better fit the teacher, while the fake model $\epsilon_{\phi_{\Theta^s}}$ uses a low-rank rotation matrix Θ^s to provide adaptive guidance. Finally, we alternate the optimization of λ_{Θ^l} and ϕ_{Θ^s} to jointly improve the quality of the generation.

Accordingly, the WaDi training objective can be rewritten from Eq. (2) as:

$$\begin{aligned} \nabla_{\lambda_{\Theta^l}} \mathcal{L}_{\text{wadi}} &= \mathbb{E}_{t,\epsilon,c} \left[\omega(t) (\epsilon_{\psi}(z_t, c, t) \right. \\ &\quad \left. - \epsilon_{\phi_{\Theta^s}}(z_t, c, t)) \frac{\partial G_{\lambda_{\Theta^l}}(z_{\text{init}}, c)}{\partial \lambda_{\Theta^l}} \right], \end{aligned} \quad (11)$$

The training objective for $\epsilon_{\phi_{\Theta^s}}$ can also be rewritten from Eq. (1) as:

$$\min_{\phi_{\Theta^s}} \mathbb{E}_{t,\epsilon,c} \|\epsilon_{\phi_{\Theta^s}}(z_t, c, t) - \epsilon\|_2^2. \quad (12)$$

4. Experiment

4.1. Experimental Setup

Evaluation Datasets and Metrics. We systematically evaluate the zero-shot text-to-image generation capability of WaDi on the COCO 2014 [32] and COCO 2017 [32] datasets, using 30k and 5k randomly sampled images, respectively. To comprehensively assess the quality of the generation, we use the Fréchet Inception Distance (FID) [14] to measure image fidelity and the CLIP score [47] to evaluate the semantic alignment of text-image. The FID is calculated using Inception V3 [62] as the feature extractor, while the CLIP score is based on the ViT-G/14 [7] model. We further adopt precision and recall [27] to evaluate fidelity and diversity. Finally, we also evaluate text-image alignment on the Human Preference Score v2 (HPSv2) [68] benchmark. See *Suppl. G.1* for details.

Implementation Details. Following prior methods [8, 43, 72, 73], the student model in WaDi adopts the same architecture as the teacher and is initialized with the teacher’s weights. WaDi is trained on 1.4 M prompts sampled from the JourneyDB [61] dataset. During training, the learning rate (LR) for the student is set to $1e-4$, while the fake model

Table 1. Quantitative comparison of WaDi and other methods on zero-shot COCO 2014 results. * indicates our reproduced results, and [†] indicates results using the official pre-trained models. ‘-’ denotes unknown. Best and second-best scores are in **bold** and underline, respectively. “Image-free” refers to training without supervision from real images.

Method	#Params	NFEs	Type	Trainable params	FID ↓	CLIP ↑	Precision ↑	Recall ↑	Image-free?	Training Data
Stable Diffusion 1.5-based backbone										
SD 1.5 (<i>cfg</i> = 3.0)	860M	25	U-Net	860M	8.78	0.30	0.59	0.53	✗	5B
LCM-LoRA [†]	860M	1	LoRA	67.50M	77.73	0.24	0.22	0.15	✗	12M
InstaFlow	860M	1	U-Net	860M	13.10	0.28	0.53	0.45	✗	3.2M
UFOGen	860M	1	U-Net	860M	12.78	-	-	-	✗	12M
DMD	860M	1	U-Net	860M	<u>11.49</u>	0.32	-	-	✗	3M
DMD2*	860M	1	U-Net	860M	12.96	0.30	<u>0.60</u>	<u>0.47</u>	✓	1.4M
SiD-LSG*	860M	1	U-Net	860M	14.27	0.30	0.56	0.48	✓	1.4M
PCM	860M	1	U-Net	860M	17.91	0.29	-	-	✗	3M
Hyper-SD [†]	860M	1	LoRA	67.25M	22.90	<u>0.31</u>	0.62	0.25	✗	-
YOSO [†]	860M	1	LoRA	67.25M	23.68	0.29	0.56	0.36	✗	4M
WaDi	860M	1	LoRaD	83.80M	10.79	<u>0.31</u>	0.62	0.48	✓	1.4M
Stable Diffusion 2.1-based backbone										
SD 2.1 (<i>cfg</i> = 3.0)	865M	1	U-Net	865M	9.60	0.32	0.59	0.50	✗	5B
SD-Turbo [†]	865M	1	U-Net	865M	16.14	0.33	0.65	0.35	✗	-
Swiftbrush	865M	1	U-Net	865M	16.67	0.29	0.47	0.46	✓	1.4M
Swiftbrushv2*	865M	1	U-Net+LoRA	884.14M	15.98	0.33	0.58	<u>0.47</u>	✓	1.4M
SiD-LSG*	865M	1	U-Net	865M	15.17	0.30	0.56	0.46	✓	1.4M
TiUE [†]	865M	1	U-Net	865M	<u>13.49</u>	<u>0.31</u>	0.59	0.48	✓	1.4M
WaDi	865M	1	LoRaD	94.43M	12.34	<u>0.31</u>	<u>0.60</u>	0.48	✓	1.4M
PixArt- α -based backbone										
PixArt- α (<i>cfg</i> = 4.5) [†]	610.86M	20	DiT	610.86M	8.75	0.32	0.75	0.45	✗	25M
Swiftbrush*	610.86M	1	DiT	610.86M	29.89	<u>0.28</u>	0.50	0.26	✓	1.4M
PG-SB*	610.86M	1	DiT	610.86M	<u>25.58</u>	<u>0.28</u>	<u>0.53</u>	<u>0.27</u>	✓	1.4M
WaDi	610.86M	1	LoRaD	81.22M	18.99	0.30	0.64	0.29	✓	1.4M

uses an LR of $1e-2$. We use AdamW [36] as the optimizer, with a batch size of 128 (16 per GPU). The classifier-free guidance (CFG) scale is set to 1.5, and the training is conducted for 2 epochs. We distill student models based on three different backbones, namely SD 1.5 [49], SD 2.1 [49], and PixArt- α (256×256) [4]. For SD 1.5 and SD 2.1, the LoRaD rank of the student is set to 256, while for PixArt- α , it is set to 128. The LoRaD rank for all fake models is uniformly set to 32. See [Suppl. F.1](#) for details.

4.2. Comparison with State-of-the-Art Methods

Quantitative results. We comprehensively evaluate WaDi on the COCO 2014 dataset against SOTA zero-shot one-step generation methods across three backbones: SD 1.5, SD 2.1, and PixArt- α . To ensure fair comparison and considering computational constraints, we follow the setup of TiUE [29] and uniformly reproduce WaDi, DMD2, SiD-LSG, and SwiftBrushv2 using 1.4M prompts. As shown in Tab. 1, WaDi achieves the best FID and Recall scores on all backbones, demonstrating superior fidelity and diversity. It also ranks first or second in CLIP and Precision, indicating strong text-image alignment and perceptual quality. Notably, only 9.74%, 10.92%, and 13.30% of the model parameters are trainable for SD 1.5, SD 2.1, and PixArt- α , respectively, highlighting WaDi’s parameter efficiency. These improvements stem from our proposed LoRaD, which reparameterizes weight updates via low-rank rotations to enable stable and efficient distillation. See [Suppl. F.4, G.3](#).

Qualitative results. Fig. 4 presents a qualitative compari-

son of WaDi with SOTA one-step generation methods based on SD 1.5 and SD 2.1 backbones. Across diverse prompts, WaDi consistently produces visually coherent and semantically aligned results. For example, in the first and second rows, WaDi better preserves structure and stylistic fidelity, capturing sharp features and vibrant colors without artifacts or distortions. In the third and fourth rows, it accurately follows prompts involving specific subjects (*e.g.*, sphynx cat, corgi, shiba inu) and contexts (*e.g.*, theater, clothing), while alternative methods often miss key attributes or yield unrealistic shapes. Notably, in the last row, WaDi generates complex scenes (*e.g.*, dog looking at TV) with consistent spatial composition and background details, demonstrating superior holistic understanding compared to other baselines. See [Suppl. G.5](#).

4.3. Downstream Tasks

Controllable generation. ControlNet [74] is a widely used controllable generation model that incorporates spatial conditions into SD [49] for fine-grained control. As shown in Fig. 5, applying WaDi to ControlNet significantly improves inference efficiency, reducing inference time by **86.26%** while preserving image quality, faithfully following spatial conditions, and maintaining prompt adherence comparable to ControlNet.

Relation inversion. Reversion [22] is the first method to guide specific object relationship synthesis in SD via relational prompts. Integrating WaDi into Reversion significantly accelerates inference. As shown in Fig. 6, WaDi

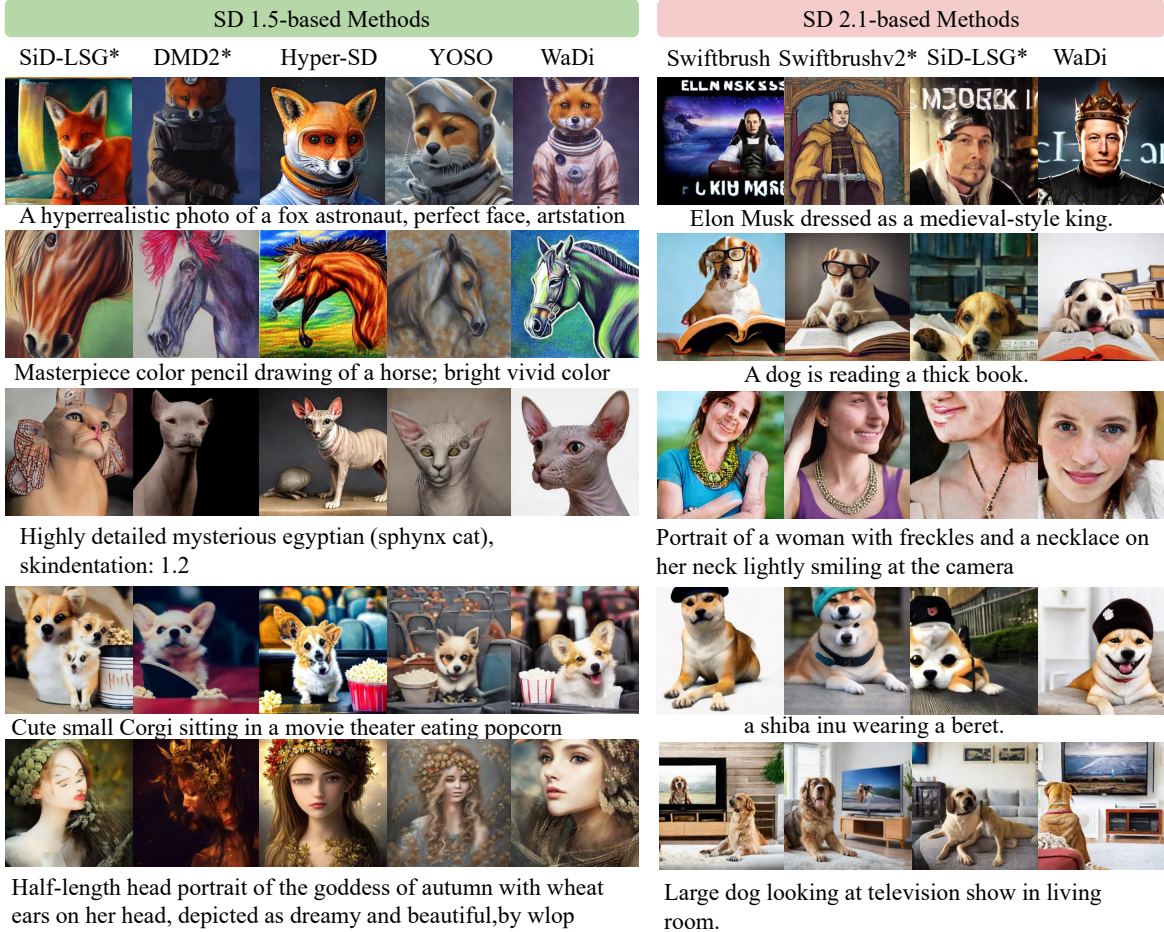


Figure 4. Qualitative comparison with other methods, where * indicates our reproduced results.

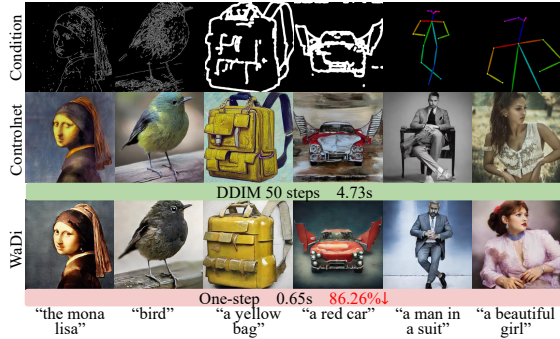


Figure 5. Quality results by Controlnet [74] with or without WaDi.

Table 2. Ablation study on the impact of adapter type in WaDi (SD 1.5, VSD loss) on the COCO 2017 dataset. “NM” and “DM” denote the norm mean and direction mean for all layers, respectively.

Type	#Params	FID	CLIP	NM	DM
LoRA	120.9M	25.27	0.29	0.06	0.83
DoRA	121.2M	26.56	0.30	0.03	0.55
DoRA (frozen norm)	120.9M	24.52	0.30	-	0.92
FT (DMD2)	860.0M	23.30	0.30	0.10	2.21
LoRaD	83.8M	20.86	0.31	-	2.89

reduces inference time by **88.89%** while producing high-fidelity images that align with the relational prompts, with quality close to that of the original multi-step Reversion. See



Figure 6. Quality results by Reversion [22] with or without WaDi.

Suppl. F.2 for more results.

Image customization. Dreambooth [50] is a pioneering personalized text-to-image framework that binds the target subject to a rare token via FT of the U-Net. To enhance parameter efficiency, we integrate our proposed LoRaD into Dreambooth and compare it with Dreambooth (FT) and LoRA [16]. As shown in Fig. 7, vanilla DreamBooth overfits by capturing the subject while memorizing training images, thus reducing prompt sensitivity. LoRA alleviates overfit-



Figure 7. Quality results by Dreambooth with or without LoRaD.

Table 3. Ablation study on the impact of the rank on WaDi (SD 1.5, VSD loss) on COCO 2014 dataset.

Setting	Rank				FID	CLIP
	Student	#Params	Fake model	#Params		
A	64	20.95M	32	9.38M	13.64	0.30
B	128	41.90M	32	9.38M	13.16	0.29
C	256	83.80M	32	9.38M	10.79	0.31
D	512	167.59M	32	9.38M	12.75	0.30
E	256	83.80M	16	4.69M	17.53	0.29
F	256	83.80M	64	18.76M	16.98	0.31

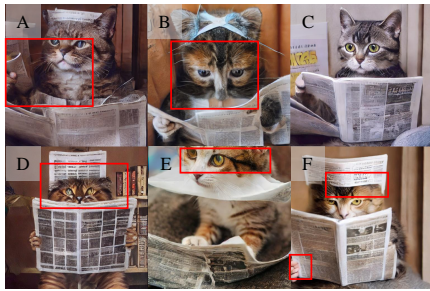


Figure 8. One-step image generation with various settings.

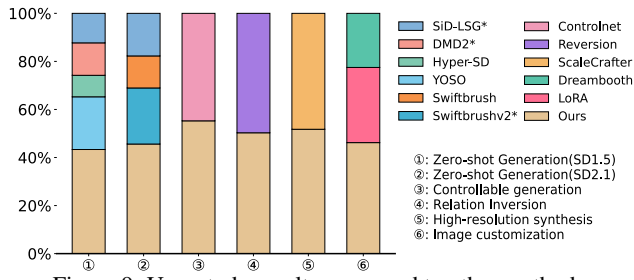


Figure 9. User study results compared to other methods.

ting, but degrades subject identity and image fidelity. In contrast, LoRaD maintains subject fidelity while adhering to prompts, achieving a better balance. We include this DreamBooth experiment only as an illustrative example, not as a comprehensive study of diffusion fine-tuning.

4.4. User Study

To evaluate image quality and text-image alignment, we conducted a user study with 57 participants, covering zero-shot generation and downstream tasks. As shown in Fig. 9, the results clearly demonstrate the superiority of our method over existing baselines. See [Suppl. F.5](#) for details.

4.5. Ablation Studies

Tab. 2 compares five adapter types on COCO 2017 under VSD loss. LoRaD achieves the lowest FID (20.86) and competitive CLIP score (0.31) with only 83.8M trainable parameters ($\sim 31\%$ fewer than LoRA/DoRA and $\sim 90\%$ fewer than FT). It also yields the highest direction mean (2.89%, vs. 2.21% for FT and $\leq 0.92\%$ for the LoRA/DoRA variants), indicating a broader and more effective update-direction space under a compact parameterization. Unlike DoRA and DoRA (frozen norm), which optimize directions via LoRA-style additive updates to normalized weights followed by **dynamic re-normalization**, LoRaD directly parameterizes **low-rank orthogonal rotations** of pre-trained weights, preserving norms and operating purely in direction space. Overall, LoRaD shows a favorable quality–efficiency trade-off.

We conduct an ablation study on COCO 2014 to assess the impact of rank configuration in WaDi. As shown in Tab. 3, we make three key observations: 1) **Increasing student rank consistently improves performance**. Raising the rank from setting A to C reduces FID from 13.64 to 10.79, indicating that higher rank enables the student to better capture the teacher’s distribution and improve generation quality. 2) **Increasing the rank beyond a threshold yields diminishing returns**. Comparing settings C and D, further increasing the rank degrades FID (12.75 vs. 10.79) and CLIP (0.31 vs. 0.30), suggesting that overly large ranks may cause overfitting. 3) **Fake model rank affects fidelity more than alignment**. Varying the fake model rank (settings C, E, F) changes FID but leaves CLIP largely stable, implying fidelity is more sensitive to capacity than alignment. In summary, setting C offers a favorable trade-off between model capacity and performance, consistent with the qualitative results in Fig. 8. See [Suppl. G.2, G.4](#) for details.

5. Conclusion

This paper presents Weight Direction-aware Distillation (WaDi), an efficient one-step text-to-image distillation framework. Through an in-depth analysis of weight changes between multi-step and one-step models, we find that changes in weight direction serve as a key mechanism in distillation, while changes in norm play a comparatively smaller role. Based on this insight, we introduce the Low-rank Rotation of weight Direction (LoRaD) module to model directional adjustments in a parameter-efficient manner. Extensive experiments demonstrate that WaDi significantly outperforms existing one-step methods—such as DMD, SiD-LSG, and SwiftBrush—in both image quality and inference speed. Moreover, the distilled model can be seamlessly adapted to a wide range of downstream tasks, showcasing strong generalization and practical applicability. Our work offers a novel theoretical perspective and practical solution for efficient diffusion model distillation.

Acknowledgement.

This work was supported by the National Science Fund of China under Grant Nos, 62361166670 and U24A20330, the “Science and Technology Yongjiang 2035” key technology breakthrough plan project (2024Z120), the Shenzhen Science and Technology Program (JCYJ20240813114237048), the Chinese government-guided local science and technology development fund projects (scientific and technological achievement transfer and transformation projects) (254Z0102G), and the Supercomputing Center of Nankai University (NKSC).

References

- [1] Armen Aghajanyan, Sonal Gupta, and Luke Zettlemoyer. Intrinsic dimensionality explains the effectiveness of language model fine-tuning. In *ACL*, pages 7319–7328, 2021. 3
- [2] Omer Bar-Tal, Hila Chefer, Omer Tov, Charles Herrmann, Roni Paiss, Shiran Zada, Ariel Ephrat, Junhwa Hur, Guanghui Liu, Amit Raj, et al. Lumiere: A space-time diffusion model for video generation. In *SIGGRAPH Asia*, pages 1–11, 2024. 2
- [3] Clement Chadebec, Onur Tasar, Eyal Benaroché, and Benjamin Aubin. Flash diffusion: Accelerating any conditional diffusion model for few steps image generation. In *AAAI*, pages 15686–15695, 2025. 2
- [4] Junsong Chen, YU Jincheng, GE Chongjian, Lewei Yao, Enze Xie, Zhongdao Wang, James Kwok, Ping Luo, Huchuan Lu, and Zhenguo Li. Pixart- α : Fast training of diffusion transformer for photorealistic text-to-image synthesis. In *ICLR*, 2023. 2, 3, 6
- [5] Junsong Chen, Chongjian Ge, Enze Xie, Yue Wu, Lewei Yao, Xiaozhe Ren, Zhongdao Wang, Ping Luo, Huchuan Lu, and Zhenguo Li. Pixart- σ : Weak-to-strong training of diffusion transformer for 4k text-to-image generation. In *ECCV*, pages 74–91. Springer, 2024.
- [6] Junsong Chen, Simian Luo, and Enze Xie. Pixart- δ : Fast and controllable image generation with latent consistency models. In *ICML*, 2024. 3
- [7] Mehdi Cherti, Romain Beaumont, Ross Wightman, Mitchell Wortsman, Gabriel Ilharco, Cade Gordon, Christoph Schuhmann, Ludwig Schmidt, and Jenia Jitsev. Reproducible scaling laws for contrastive language-image learning. In *CVPR*, pages 2818–2829, 2023. 5
- [8] Trung Dao, Thuan Hoang Nguyen, Thanh Le, Duc Vu, Khoi Nguyen, Cuong Pham, and Anh Tran. Swiftbrush v2: Make your one-step diffusion model better than its teacher. In *ECCV*, pages 176–192. Springer, 2024. 2, 3, 5
- [9] Yanjie Dong, Haijun Zhang, Chengming Li, Song Guo, Victor Leung, and Xiping Hu. Fine-tuning and deploying large language models over edges: Issues and approaches. *arXiv preprint arXiv:2408.10691*, 2024. 3
- [10] Patrick Esser, Sumith Kulal, Andreas Blattmann, Rahim Entezari, Jonas Müller, Harry Saini, Yam Levi, Dominik Lorenz, Axel Sauer, Frederic Boesel, et al. Scaling rectified flow transformers for high-resolution image synthesis. In *ICML*, 2024. 3
- [11] Shanghua Gao, Pan Zhou, Ming-Ming Cheng, and Shuicheng Yan. Towards sustainable self-supervised learning: Target-enhanced conditional mask-reconstruction for self-supervised learning. *Scientia Sinica Informationis*, 55(2):326–342, 2025. 3
- [12] Zeyu Han, Chao Gao, Jinyang Liu, Jeff Zhang, and Sai Qian Zhang. Parameter-efficient fine-tuning for large models: A comprehensive survey. *TMLR*, 2024. 3
- [13] Soufiane Hayou, Nikhil Ghosh, and Bin Yu. The impact of initialization on lora finetuning dynamics. *NeurIPS*, 37: 117015–117040, 2024. 3
- [14] Martin Heusel, Hubert Ramsauer, Thomas Unterthiner, Bernhard Nessler, and Sepp Hochreiter. Gans trained by a two time-scale update rule converge to a local nash equilibrium. *NeurIPS*, 30, 2017. 5
- [15] Jonathan Ho, Ajay Jain, and Pieter Abbeel. Denoising diffusion probabilistic models. *NeurIPS*, 33:6840–6851, 2020. 1, 3
- [16] Edward J Hu, Yelong Shen, Phillip Wallis, Zeyuan Allen-Zhu, Yuanzhi Li, Shean Wang, Lu Wang, Weizhu Chen, et al. Lora: Low-rank adaptation of large language models. *ICLR*, 1(2):3, 2022. 2, 4, 5, 7
- [17] Xiantao Hu, Ying Tai, Xu Zhao, Chen Zhao, Zhenyu Zhang, Jun Li, Bineng Zhong, and Jian Yang. Exploiting multimodal spatial-temporal patterns for video object tracking. In *AAAI*, pages 3581–3589, 2025. 3
- [18] Xiantao Hu, Bineng Zhong, Qihua Liang, Liangtao Shi, Zhiyi Mo, Ying Tai, and Jian Yang. Adaptive perception for unified visual multi-modal object tracking. *TAI*, 2025. 3
- [19] Yaosi Hu, Zhenzhong Chen, and Chong Luo. Lamd: Latent motion diffusion for image-conditional video generation. *IJCV*, pages 1–17, 2025. 2
- [20] Qiushi Huang, Tom Ko, Lilian Tang, and Yu Zhang. Comlora: A competitive learning approach for enhancing lora. In *ICLR*, 2025. 3
- [21] Tiansheng Huang, Sihao Hu, Fatih Ilhan, Selim Furkan Tekin, and Ling Liu. Lazy safety alignment for large language models against harmful fine-tuning. *arXiv preprint arXiv:2405.18641*, 2, 2024. 3
- [22] Ziqi Huang, Tianxing Wu, Yuming Jiang, Kelvin CK Chan, and Ziwei Liu. Reversion: Diffusion-based relation inversion from images. In *SIGGRAPH Asia*, pages 1–11, 2024. 6, 7
- [23] Minguk Kang, Richard Zhang, Connelly Barnes, Sylvain Paris, Suha Kwak, Jaesik Park, Eli Shechtman, Jun-Yan Zhu, and Taesung Park. Distilling diffusion models into conditional gans. In *ECCV*, pages 428–447. Springer, 2024. 3
- [24] Levon Khachatryan, Andranik Movsisyan, Vahram Tadevosyan, Roberto Henschel, Zhangyang Wang, Shant Navasardyan, and Humphrey Shi. Text2video-zero: Text-to-image diffusion models are zero-shot video generators. In *ICCV*, pages 15954–15964, 2023. 2
- [25] Dongjun Kim, Chieh-Hsin Lai, Wei-Hsiang Liao, Naoki Murata, Yuhta Takida, Toshimitsu Uesaka, Yutong He, Yuki Mitsufuji, and Stefano Ermon. Consistency trajectory models: Learning probability flow ode trajectory of diffusion. In *ICLR*, 2023. 3

- [26] Weijie Kong, Qi Tian, Zijian Zhang, Rox Min, Zuozhuo Dai, Jin Zhou, Jiangfeng Xiong, Xin Li, Bo Wu, Jianwei Zhang, et al. Hunyuanvideo: A systematic framework for large video generative models. *arXiv preprint arXiv:2412.03603*, 2024. 2
- [27] Tuomas Kynkäänniemi, Tero Karras, Samuli Laine, Jaakko Lehtinen, and Timo Aila. Improved precision and recall metric for assessing generative models. *NeurIPS*, 32, 2019. 5
- [28] Senmao Li, Taihang Hu, Joost van de Weijer, Fahad Shahbaz Khan, Tao Liu, Linxuan Li, Shiqi Yang, Yaxing Wang, Ming-Ming Cheng, et al. Faster diffusion: Rethinking the role of the encoder for diffusion model inference. *NeurIPS*, 37:85203–85240, 2024. 3
- [29] Senmao Li, Lei Wang, Kai Wang, Tao Liu, Jiehang Xie, Joost van de Weijer, Fahad Shahbaz Khan, Shiqi Yang, Yaxing Wang, and Jian Yang. One-way ticket: Time-independent unified encoder for distilling text-to-image diffusion models. In *CVPR*, pages 23563–23574, 2025. 6
- [30] Zhen Li, Mingdeng Cao, Xintao Wang, Zhongang Qi, Ming-Ming Cheng, and Ying Shan. Photomaker: Customizing realistic human photos via stacked id embedding. In *CVPR*, pages 8640–8650, 2024. 2, 3
- [31] Shanchuan Lin, Anran Wang, and Xiao Yang. Sdxl-lightning: Progressive adversarial diffusion distillation. *arXiv preprint arXiv:2402.13929*, 2024. 2, 3
- [32] Tsung-Yi Lin, Michael Maire, Serge Belongie, James Hays, Pietro Perona, Deva Ramanan, Piotr Dollár, and C Lawrence Zitnick. Microsoft coco: Common objects in context. In *ECCV*, pages 740–755. Springer, 2014. 3, 5
- [33] Luping Liu, Yi Ren, Zhijie Lin, and Zhou Zhao. Pseudo numerical methods for diffusion models on manifolds. In *ICLR*, 2022. 3
- [34] Shih-Yang Liu, Chien-Yi Wang, Hongxu Yin, Pavlo Molchanov, Yu-Chiang Frank Wang, Kwang-Ting Cheng, and Min-Hung Chen. Dora: Weight-decomposed low-rank adaptation. In *ICML*, 2024. 2
- [35] Ilya Loshchilov and Frank Hutter. Decoupled weight decay regularization. *arXiv preprint arXiv:1711.05101*, 2017. 2
- [36] Ilya Loshchilov and Frank Hutter. Decoupled weight decay regularization. In *ICLR*, 2019. 6
- [37] Cheng Lu, Yuhao Zhou, Fan Bao, Jianfei Chen, Chongxuan Li, and Jun Zhu. Dpm-solver: A fast ode solver for diffusion probabilistic model sampling in around 10 steps. *NeurIPS*, 35:5775–5787, 2022. 3
- [38] Cheng Lu, Yuhao Zhou, Fan Bao, Jianfei Chen, Chongxuan Li, and Jun Zhu. Dpm-solver++: Fast solver for guided sampling of diffusion probabilistic models. *arXiv preprint arXiv:2211.01095*, 2022. 3
- [39] Simian Luo, Yiqin Tan, Longbo Huang, Jian Li, and Hang Zhao. Latent consistency models: Synthesizing high-resolution images with few-step inference. *arXiv preprint arXiv:2310.04378*, 2023. 3
- [40] Simian Luo, Yiqin Tan, Suraj Patil, Daniel Gu, Patrick von Platen, Apolinário Passos, Longbo Huang, Jian Li, and Hang Zhao. Lcm-lora: A universal stable-diffusion acceleration module. *arXiv preprint arXiv:2311.05556*, 2023. 2, 3
- [41] Yihong Luo, Xiaolong Chen, Xinghua Qu, Tianyang Hu, and Jing Tang. You only sample once: Taming one-step text-to-image synthesis by self-cooperative diffusion gans. *arXiv preprint arXiv:2403.12931*, 2024. 3
- [42] Xinyin Ma, Gongfan Fang, and Xinchao Wang. Deepcache: Accelerating diffusion models for free. In *CVPR*, pages 15762–15772, 2024. 3
- [43] Thuan Hoang Nguyen and Anh Tran. Swiftbrush: One-step text-to-image diffusion model with variational score distillation. In *CVPR*, pages 7807–7816, 2024. 3, 4, 5
- [44] Haomiao Ni, Changhao Shi, Kai Li, Sharon X Huang, and Martin Renqiang Min. Conditional image-to-video generation with latent flow diffusion models. In *CVPR*, pages 18444–18455, 2023. 2
- [45] William Peebles and Saining Xie. Scalable diffusion models with transformers. In *ICCV*, pages 4195–4205, 2023. 3
- [46] Dustin Podell, Zion English, Kyle Lacey, Andreas Blattmann, Tim Dockhorn, Jonas Müller, Joe Penna, and Robin Rombach. Sdxl: Improving latent diffusion models for high-resolution image synthesis. In *ICLR*, 2023. 3
- [47] Alec Radford, Jong Wook Kim, Chris Hallacy, Aditya Ramesh, Gabriel Goh, Sandhini Agarwal, Girish Sastry, Amanda Askell, Pamela Mishkin, Jack Clark, et al. Learning transferable visual models from natural language supervision. In *ICML*, pages 8748–8763. Pmlr, 2021. 5
- [48] Yuxi Ren, Xin Xia, Yanzuo Lu, Jiacheng Zhang, Jie Wu, Pan Xie, XING WANG, and Xuefeng Xiao. Hyper-sd: Trajectory segmented consistency model for efficient image synthesis. In *NeurIPS*, 2024. 2, 3
- [49] Robin Rombach, Andreas Blattmann, Dominik Lorenz, Patrick Esser, and Björn Ommer. High-resolution image synthesis with latent diffusion models. In *CVPR*, pages 10684–10695, 2022. 2, 3, 6
- [50] Nataniel Ruiz, Yuanzhen Li, Varun Jampani, Yael Pritch, Michael Rubinstein, and Kfir Aberman. Dreambooth: Fine tuning text-to-image diffusion models for subject-driven generation. In *CVPR*, pages 22500–22510, 2023. 2, 3, 7
- [51] Tim Salimans and Jonathan Ho. Progressive distillation for fast sampling of diffusion models. In *ICLR*, 2022. 3
- [52] Tim Salimans and Durk P Kingma. Weight normalization: A simple reparameterization to accelerate training of deep neural networks. *NeurIPS*, 29, 2016. 2
- [53] Pratheba Selvaraju, Tianyu Ding, Tianyi Chen, Ilya Zharkov, and Luming Liang. Fora: Fast-forward caching in diffusion transformer acceleration. *arXiv preprint arXiv:2407.01425*, 2024. 3
- [54] Shitong Shao, Hongwei Yi, Hanzhong Guo, Tian Ye, Daquan Zhou, Michael Lingelbach, Zhiqiang Xu, and Zeke Xie. Mag-icdistillation: Weak-to-strong video distillation for large-scale few-step synthesis. *arXiv preprint arXiv:2503.13319*, 2025. 3
- [55] Jascha Sohl-Dickstein, Eric Weiss, Niru Maheswaranathan, and Surya Ganguli. Deep unsupervised learning using nonequilibrium thermodynamics. In *ICML*, pages 2256–2265. pmlr, 2015. 1, 3
- [56] Jiaming Song, Chenlin Meng, and Stefano Ermon. Denoising diffusion implicit models. In *ICLR*, 2021. 3
- [57] Yang Song and Stefano Ermon. Generative modeling by estimating gradients of the data distribution. *NeurIPS*, 32, 2019. 3

- [58] Yang Song, Jascha Sohl-Dickstein, Diederik P Kingma, Abhishek Kumar, Stefano Ermon, and Ben Poole. Score-based generative modeling through stochastic differential equations. In *ICLR*, 2021. 1, 3
- [59] Yang Song, Prafulla Dhariwal, Mark Chen, and Ilya Sutskever. Consistency models. In *ICML*, pages 32211–32252. PMLR, 2023. 3
- [60] Jianlin Su, Murtadha Ahmed, Yu Lu, Shengfeng Pan, Wen Bo, and Yunfeng Liu. Roformer: Enhanced transformer with rotary position embedding. *Neurocomputing*, 568:127063, 2024. 4
- [61] Keqiang Sun, Junting Pan, Yuying Ge, Hao Li, Haodong Duan, Xiaoshi Wu, Renrui Zhang, Aojun Zhou, Zipeng Qin, Yi Wang, et al. Journeydb: A benchmark for generative image understanding. *NeurIPS*, 36:49659–49678, 2023. 5
- [62] Christian Szegedy, Vincent Vanhoucke, Sergey Ioffe, Jon Shlens, and Zbigniew Wojna. Rethinking the inception architecture for computer vision. In *CVPR*, pages 2818–2826, 2016. 5
- [63] Ang Wang, Baole Ai, Bin Wen, Chaojie Mao, Chen-Wei Xie, Di Chen, Feiwu Yu, Haiming Zhao, Jianxiao Yang, Jianyuan Zeng, et al. Wan: Open and advanced large-scale video generative models. *arXiv preprint arXiv:2503.20314*, 2025. 2
- [64] Fu-Yun Wang, Zhaoyang Huang, Alexander Bergman, Dazhong Shen, Peng Gao, Michael Lingelbach, Keqiang Sun, Weikang Bian, Guanglu Song, Yu Liu, et al. Phased consistency models. *NeurIPS*, 37:83951–84009, 2024. 3
- [65] Zhengyi Wang, Cheng Lu, Yikai Wang, Fan Bao, Chongxuan Li, Hang Su, and Jun Zhu. Prolificdreamer: High-fidelity and diverse text-to-3d generation with variational score distillation. *NeurIPS*, 36:8406–8441, 2023. 3, 4
- [66] Felix Wimbauer, Bichen Wu, Edgar Schoenfeld, Xiaoliang Dai, Ji Hou, Zijian He, Artsiom Sanakoyeu, Peizhao Zhang, Sam Tsai, Jonas Kohler, et al. Cache me if you can: Accelerating diffusion models through block caching. In *CVPR*, pages 6211–6220, 2024. 3
- [67] Jay Zhangjie Wu, Yixiao Ge, Xintao Wang, Stan Weixian Lei, Yuchao Gu, Yufei Shi, Wynne Hsu, Ying Shan, Xiaohu Qie, and Mike Zheng Shou. Tune-a-video: One-shot tuning of image diffusion models for text-to-video generation. In *ICCV*, pages 7623–7633, 2023. 2
- [68] Xiaoshi Wu, Yiming Hao, Keqiang Sun, Yixiong Chen, Feng Zhu, Rui Zhao, and Hongsheng Li. Human preference score v2: A solid benchmark for evaluating human preferences of text-to-image synthesis. *arXiv preprint arXiv:2306.09341*, 2023. 5
- [69] Yu-Huan Wu, Da Zhang, Le Zhang, Xin Zhan, Dengxin Dai, Yun Liu, and Ming-Ming Cheng. Ret3d: Rethinking object relations for efficient 3d object detection in driving scenes. *Scientia Sinica Informationis*, 55(2):326–342, 2025. 3
- [70] Yanwu Xu, Yang Zhao, Zhisheng Xiao, and Tingbo Hou. Ufo-gen: You forward once large scale text-to-image generation via diffusion gans. In *CVPR*, pages 8196–8206, 2024. 3
- [71] Hongwei Yi, Shitong Shao, Tian Ye, Jiantong Zhao, Qingyu Yin, Michael Lingelbach, Li Yuan, Yonghong Tian, Enze Xie, and Daquan Zhou. Magic 1-for-1: Generating one minute video clips within one minute. *arXiv preprint arXiv:2502.07701*, 2025. 3
- [72] Tianwei Yin, Michaël Gharbi, Taesung Park, Richard Zhang, Eli Shechtman, Fredo Durand, and Bill Freeman. Improved distribution matching distillation for fast image synthesis. *NeurIPS*, 37:47455–47487, 2024. 2, 3, 4, 5
- [73] Tianwei Yin, Michaël Gharbi, Richard Zhang, Eli Shechtman, Fredo Durand, William T Freeman, and Taesung Park. One-step diffusion with distribution matching distillation. In *CVPR*, pages 6613–6623, 2024. 2, 3, 4, 5
- [74] Lvmin Zhang, Anyi Rao, and Maneesh Agrawala. Adding conditional control to text-to-image diffusion models. In *ICCV*, pages 3836–3847, 2023. 2, 3, 6, 7
- [75] Qinsheng Zhang and Yongxin Chen. Fast sampling of diffusion models with exponential integrator. In *NeurIPS 2022 Workshop on Score-Based Methods*, 2022. 3
- [76] Mingyuan Zhou, Zhendong Wang, Huangjie Zheng, and Hai Huang. Long and short guidance in score identity distillation for one-step text-to-image generation. *arXiv preprint arXiv:2406.01561*, 2024. 3, 4
- [77] Mingyuan Zhou, Huangjie Zheng, Zhendong Wang, Mingzhang Yin, and Hai Huang. Score identity distillation: Exponentially fast distillation of pretrained diffusion models for one-step generation. In *ICML*, 2024. 4
- [78] Yupeng Zhou, Daquan Zhou, Ming-Ming Cheng, Jiashi Feng, and Qibin Hou. Storydiffusion: Consistent self-attention for long-range image and video generation. *NeurIPS*, 37:110315–110340, 2024. 2